

## HYDROGEN ABSORPTION INTO ALPHA TITANIUM ALLOYS

L. Yan, J. J. Noël, D. W. Shoesmith

Chemistry Department, University of Western Ontario, London, ON, Canada, N6A 5B7

### Abstract

Hydrogen absorption into titanium alloys during crevice corrosion has been studied in  $0.27 \text{ mol/cm}^3$  at  $95^\circ\text{C}$ . Experiments of different durations were performed to investigate the progression of crevice corrosion and hydrogen absorption. It was found that the main driving force for crevice corrosion processes was proton reduction inside the crevice rather than  $\text{O}_2$  reduction on the counter electrode. The data also showed that the amount of absorbed hydrogen and the maximum penetration depth increased with time.

### Introduction

Hydrogen absorption leading to hydrogen-induced cracking (HIC) is a well documented mode of failure for titanium alloys. For failure by HIC to occur, corrosion must lead to absorption into the alloy of substantial quantities of hydrogen. Hydrogen can be absorbed into Ti alloys by two routes: (a) via crevice corrosion, when the unprotected nature of the corroding surface allows hydrogen to be absorbed relatively rapidly; (b) via passive corrosion, when hydrogen absorption will be slow because of the presence of an oxide film. Here we focus primarily on hydrogen absorption under crevice corrosion conditions.

Hydrogen absorption can be quantified as a hydrogen uptake or absorption efficiency. This quantity can be defined as the fraction of the hydrogen produced electrolytically, or by corrosion, that is absorbed into the metal [1]. The key factors that affect hydrogen absorption are the following:

i) The alloy microstructure;

Hydrogen has different solubilities in different phases (i.e., the  $\alpha$ - and  $\beta$ - phases) in Ti alloys. At room temperature the solubility of hydrogen in the alpha phase is of the order of  $20\sim 200 \mu\text{g/g}$ , but much higher in the beta-phase. For example, more than  $4000 \mu\text{g/g}$  hydrogen is soluble in Ti-20% Mo alloy (a  $\beta$ - phase Ti alloy) at room temperature [2].

ii) Alloying additions (Ni, Mo, Pd) and impurities (Fe);

Previous work [3-7] has shown that alloy additions and impurities exist in the metal as either interstitial atoms, intermetallic precipitates or both. These interstitial atoms and precipitates can catalyze proton reduction and also serve as hydrogen absorption windows.

iii) pH;

Schutz [8], Phillips [9], and Okada [10] observed a decrease in hydrogen absorption with an increasing solution pH,

iv) The presence of an oxide film;

It has been found that oxide films on titanium alloys are highly impermeable to hydrogen [10-11].

v) Temperature;

Phillips reported that in the range  $25$  to  $100^\circ\text{C}$ , the rate of hydrogen absorption increased parabolically with temperature [9];

vi) Surface preparation [9].

Qin and Shoosmith [12] have developed a model to predict when failures caused by HIC in the drip shields proposed for the Yucca Mountain nuclear waste repository might occur. This model conservatively assumes that absorbed hydrogen is immediately distributed throughout the alloy. However, it only takes into account hydrogen produced by general corrosion, and does not include the possibility that a period of crevice corrosion, while not challenging the integrity of the structure by wall penetration, could lead to a significant amount of hydrogen absorption. Our primary goal is to improve this model by modifying some of the over-simplified assumptions used, and by measuring improved values for the key modelling parameters. In this paper we present the results of some experimental studies conducted under crevice corrosion conditions.

## Experimental

### Experimental cells

The cell for crevice corrosion is shown schematically in Fig. 1. The cell was built inside a pressure vessel (Parr Instrument Co., model 4621). The lid was made to accept four sealing glands for electrode feed-throughs. The working electrode was galvanically coupled to the large surface area counter electrode ( $\sim 50$  times the surface area of the working electrode) by a zero-resistance ammeter (Keithley, model 6514). The cylinder-shaped counter electrode had the same composition as the working electrode. A homemade Ag/AgCl ( $0.1 \text{ mol}\cdot\text{L}^{-1}$  KCl) reference electrode was used to measure the potential. The planar working electrode was a rectangular prism  $20 \text{ mm} \times 5 \text{ mm} \times 5 \text{ mm}$ , of the same material as the working electrode. The potential of the planar electrode was monitored using the same reference electrode.

### Working electrode

The working electrode for crevice corrosion comprises two coupons, one cut from the Ti-2 plate, the other from a 14 mm thick polysulfone plate. Crevice coupons had nominal dimensions of  $50 \text{ mm} \times 22 \text{ mm} \times$  thickness of the material. A small PTFE crevice former,  $25 \text{ mm} \times 15 \text{ mm} \times 1.6 \text{ mm}$ , was sandwiched between the crevice coupons, defining the creviced area on the specimen. All the bolts and nuts for the working electrode were fabricated from the same Ti-2 plate as the crevice coupon to avoid any galvanic coupling.

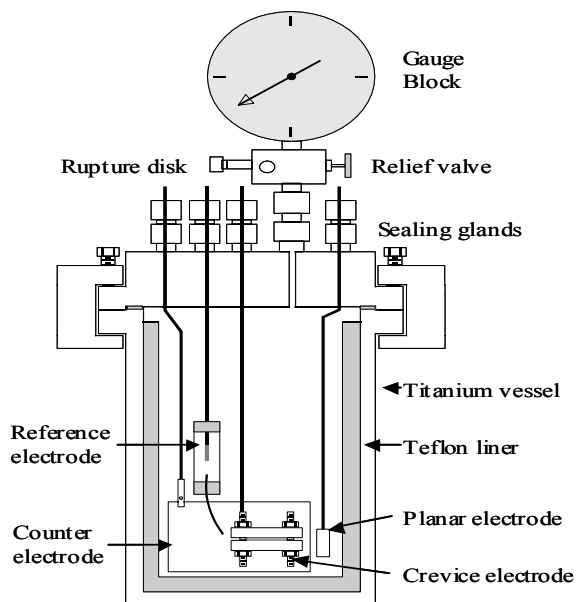


Fig. 1 Schematic diagram of the crevice corrosion cell [13]

## Experimental solutions

All the crevice corrosion experiments were performed in a solution of  $0.27 \text{ mol}\cdot\text{L}^{-1}$  NaCl at  $95^\circ\text{C}$ . The solution was aerated by vigorous agitation in air. The pressure of the cell was brought up to 60 psi with Ar to suppress boiling of the solution.

## Material compositions

All of the electrodes for crevice corrosion experiments were from the same Ti-2 plate. The chemical composition of this Ti-2 plate is shown in Table 1:

**Table 1** Composition (wt%) of Ti Grade-2 used in the experiments

|      | Fe    | C     | O     | N     | Ni    | Ti   |
|------|-------|-------|-------|-------|-------|------|
| Ti-2 | 0.107 | 0.010 | 0.127 | 0.010 | 0.023 | Bal. |

## Hydrogen Analysis

The hydrogen content in the metal was measured using a RH-404 hydrogen Determinator (LECO Corporation). In this apparatus, a high temperature is applied to melt the metal and drive off gases present in the sample material. Hydrogen and other gases are swept away by a carrier gas stream of Ar. The undesirable materials are removed from the carrier gas using a series of particle and chemical filters. Finally, the gases are separated in a molecular sieve column. Hydrogen, with the lowest molecular weight, passes through the column much faster than other heavier gases. After the molecular sieve column, hydrogen is detected and analyzed in a thermal conductivity cell. The accuracy of this technique is  $\pm 0.05 \mu\text{g/g}$  or  $\pm 2\%$  of a reading, and the precision is  $\pm 0.01 \mu\text{g/g}$  or  $0.1\%$  of a reading (whichever is greater).

## Weight change, oxygen and hydrogen consumption measurement

On completion of a crevice corrosion experiment, the whole crevice working electrode was dried in a desiccator until three consecutive weighings gave masses within  $\pm 0.5 \text{ mg}$ . The weight gained was used to determine the total extent of corrosion. Crevice corrosion has two contributions: one caused by external  $\text{O}_2$  reduction on the counter electrode, the other by internal  $\text{H}^+$  reduction. Since H is much lighter than O, the weight gain is due overwhelmingly to oxide formation (i.e., the formation of hydride was ignored). The total weight was converted to charge units (Q) using Faraday's law.

The extent of corrosion driven by external  $\text{O}_2$  reduction ( $Q_{\text{O}_2}$ ), was determined by integrating the coupled crevice current over time. The ratio  $Q_{\text{O}_2}/Q$  represented the fraction of the corrosion driven by external  $\text{O}_2$  reduction. Accordingly, the corrosion driven by proton reduction ( $Q_{\text{H}_2}$ ) was described by the difference between  $Q_{\text{O}_2}$  and Q.

After the weight measurement the crevice coupons were cut in half, one for hydrogen analysis and the other one for penetration depth measurement.

## Results and discussion

Fig. 2 shows the crevice current ( $I_c$ ), crevice potential ( $E_c$ ) and planar potential ( $E_p$ ) recorded in  $0.27 \text{ mol}\cdot\text{L}^{-1}$  NaCl at  $95^\circ\text{C}$  with different experimental durations. Very reproducible behaviour was observed. Since Ti oxidation and  $\text{H}^+$  reduction occur on the same Ti working electrode, the reaction is short-circuited and no current for  $\text{H}^+$  reduction is detected. The crevice current shown in Fig. 2 was the contribution from external  $\text{O}_2$  reduction on the counter electrode.

A planar electrode was used to detect the potential of the uncreviced Ti-2 material. The difference between the planar and crevice potentials is a measurement of driving force for crevice corrosion. The planar potentials showed that 2~3 days were needed to grow the oxide

film on the surface to the passivated steady state. For all experimental durations, the planar potential showed consistent and stable values ( $\sim 0.3 \text{ V}_{\text{vs Ag/AgCl}}$ ), indicating that the reference electrode was performing well at  $95^\circ\text{C}$ .

The initiation time for crevice corrosion was quite reproducible and around 2 days, consistent with previous research [14,15]. On initiation, the crevice current showed a quick surge in magnitude, accompanied by a drop in crevice potential. A peak was observed during the early propagation period (2~10 days) for all the experiments. This observation was in accord with He's [15] results, and attributed to activation of corrosion sites around the perimeter of the creviced area, which required significant external  $\text{O}_2$  reduction currents. These sites are the easiest to couple to the counter electrode because of the low IR effect. Images of the damage incurred during the shortest experiment (12.82 days), Fig. 3, show more damage occurring along the edges of the crevice.

The maximum crevice currents were within the range of  $150\sim 200 \mu\text{A}$ , except for the experiment lasting 41.76 days ( $\sim 250 \mu\text{A}$ ). The calculated data (Table 2) also confirmed the 41.76 day sample was corroded more than the others. During the steady propagation period, all the crevice potentials reached a stable value, around  $-250 \text{ mV}_{\text{vs Ag/AgCl}}$ . The crevice currents were not as stable as the crevice potentials, but also reached a quite stable value of  $\sim 100 \mu\text{A}$ . This confirmed the point that the cathodic current was the combination of  $\text{H}^+$  and  $\text{O}_2$  reduction. Even if the current from  $\text{O}_2$  and  $\text{H}^+$  reduction changed, as long as their sum remained the same, the crevice potential would not change. Repassivation of the crevice system did not occur even after 50 days.

The calculated crevice corrosion parameters are shown in Table 2. The increase in weight gain indicated that crevice corrosion damage accumulated with time. The amount of crevice corrosion supported by external  $\text{O}_2$  reduction ( $Q_{\text{O}_2}$ ) increased continuously with duration, but the fraction ( $Q_{\text{O}_2}/Q$ ) remained virtually unchanged with time. The data also shows that more than 70% of the crevice corrosion was supported by internal  $\text{H}^+$  reduction. The total amount of absorbed hydrogen ( $H_{\text{abs}}$ ) accumulated steadily with duration. However, the hydrogen absorption efficiency (i.e.,  $C_{\text{Habs}}$  at 12.82, 22.75, 34.36 and 51.32 days) did not change much with duration, which suggested that the hydrogen absorption process was controlled by diffusion of hydrogen deeper into the alloy, instead of adsorption of H atoms on the surface.

The results for 41.76 day sample are an interesting set of data. Weight gain (W) and charge (Q) are the largest of any experiment. Inspection of the  $I_c$ -time plot indicates this is primarily due to the high current over the first 5 to 10 days. Coincidentally the maximum penetration is greatest on this specimen and the site of maximum penetration is located at the edge. This suggests a site initiated early at the edge and probably grew for the duration of the experiment. While the amount of  $H_{\text{abs}}$  is in line with the steady accumulation of damage the  $H_{\text{abs}}$  efficiency is not. This would be consistent with a more extensive metal dissolution process at this site since dissolution would simultaneously remove surface hydride thereby accounting for the lower  $H_{\text{abs}}$  efficiency.

The penetration depth profiles of corroded coupons (Fig. 3) showed that the corrosion damage was widely distributed across the surface at shallow depths (i.e., 0 and  $30 \mu\text{m}$ ). The corroded area decreased rapidly with depth, and only a small number of individual sites were corroded to a significant depth ( $> 400 \mu\text{m}$ ) (Fig. 3 and Fig. 4). The deepest penetration was always found at the edge of the crevice (Fig. 3), i.e., at the sites that were most easily coupled to the counter electrode.

The penetration depth appears to approach a plateau with time (Fig. 5). Fig.5 also shows the comparison of the maximum penetration depth in Ti-2 with 0.078 wt% Fe [15] and 0.107 wt% Fe (the material used in this paper). Ti-2 with 0.078 wt% Fe crevice corrodes to a much higher maximum penetration depth, which is almost triple the value for Ti-2 with 0.107 wt% Fe. A possible explanation for the different behaviours is the different Fe distributions in the Ti-2 specimens. For Ti-2 with 0.078 wt% Fe, the iron is mainly present in intergranular  $\beta$ -phase. However, iron in Ti-2 with 0.107 wt% may be present as  $Ti_xFe$  particles which can act as catalytic sites for the proton reduction. This would regulate the pH at individual propagating sites, thereby slowing propagation and enforcing repassivation.

**Table 2** Crevice corrosion data for Ti-2 recorded in 0.27mol/dm<sup>3</sup> solution at 95°C with different durations

| Duration (days)                                       | 12.82  | 22.75  | 34.36  | 41.76  | 51.32  |
|---|--------|--------|--------|--------|--------|
| Max. penetrated depth ( $\mu\text{m}$ )               | 217    | 458    | 579    | 815    | 647    |
| Weight change W (g)                                   | 0.0380 | 0.0764 | 0.0815 | 0.1416 | 0.1197 |
| Charge Q (C)  | 458.4  | 921.6  | 983.1  | 1708.1 | 1445.1 |
| $Q_{O_2}$ (C)   | 118.1  | 221.7  | 307.4  | 401.0  | 462.0  |
| $Q_{O_2}/Q$ (%)                                       | 25.76  | 24.06  | 31.27  | 23.48  | 31.97  |
| $Q_{H_2}/Q$ (%)                                       | 74.24  | 75.94  | 68.73  | 76.52  | 68.03  |
| $H_{\text{abs}}$ (mg)                                 | 0.256  | 0.494  | 0.548  | 0.638  | 0.815  |
| $C_{H_{\text{abs}}}$ ( $H_{\text{abs}}/Q_{H_2}$ ) (%) | 7.27   | 6.81   | 7.82   | 4.71   | 7.99   |
| $R_{H_{\text{abs}}}$ (mg/day)                         | 0.0200 | 0.0217 | 0.0159 | 0.0153 | 0.0159 |

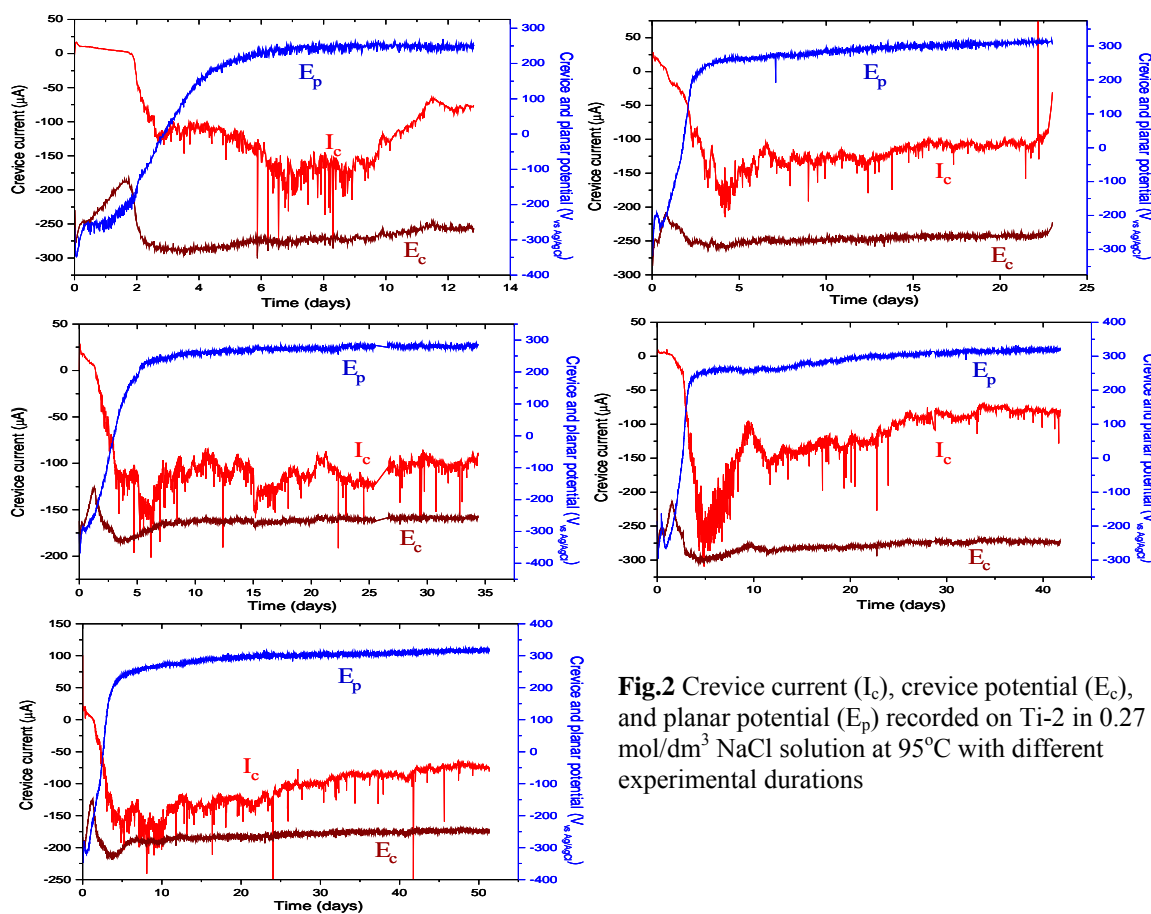


**Fig.2** Crevice current ( $I_c$ ), crevice potential ( $E_c$ ), and planar potential ( $E_p$ ) recorded on Ti-2 in 0.27 mol/dm<sup>3</sup> NaCl solution at 95°C with different experimental durations

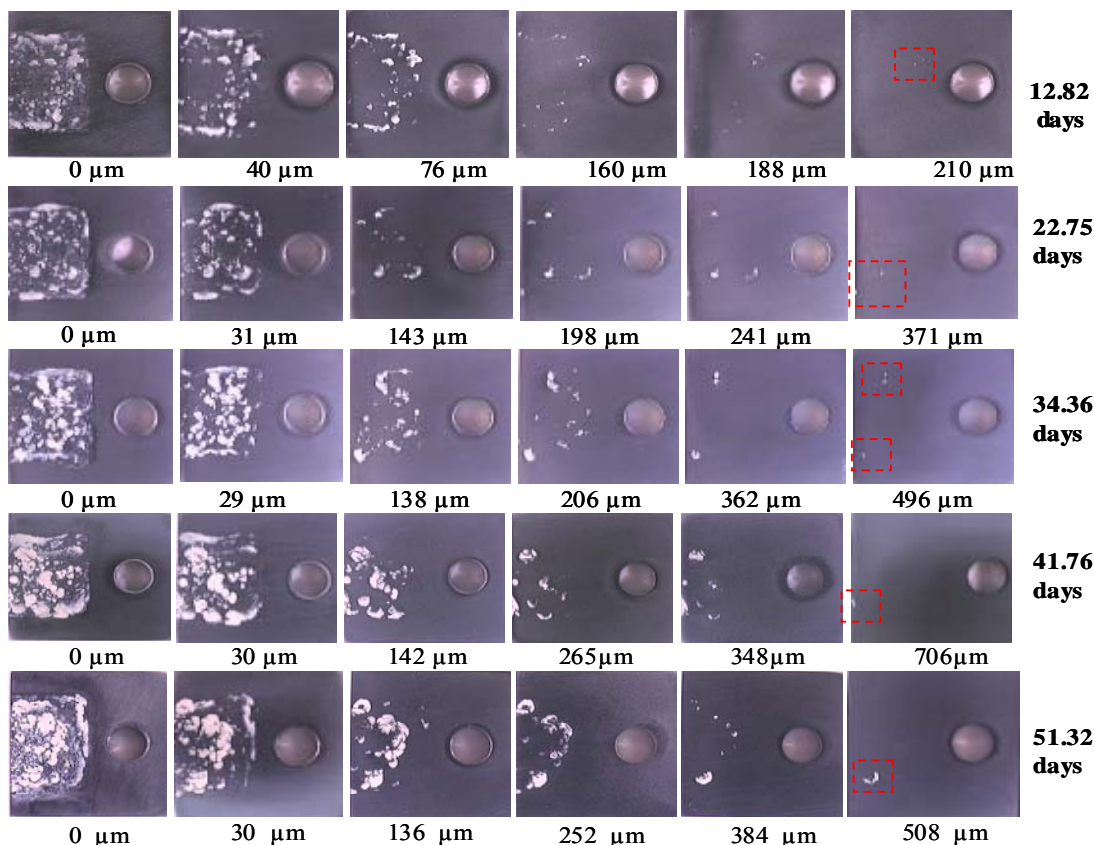


Fig. 3 Depth profiles of the corroded coupons for 12.82, 22.75, 34.36, 41.76 and 51.32 days, respectively

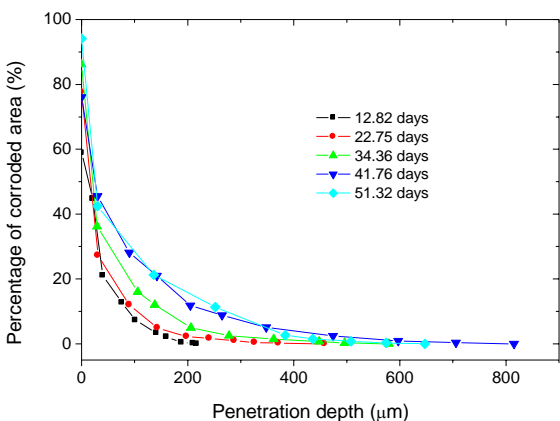


Fig. 4 percentage of the crevice area corroded as a function of penetration depth at 95°C in 0.27 mol/dm<sup>3</sup> NaCl solution

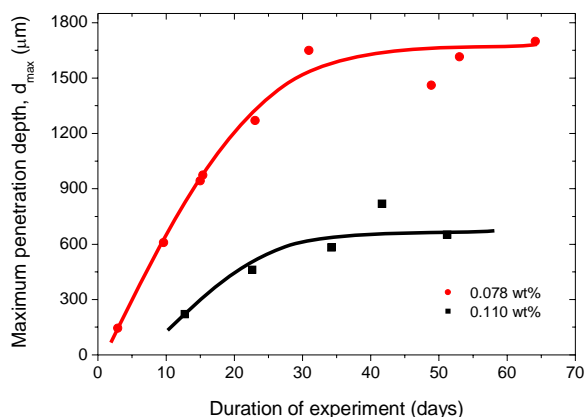


Fig. 5 Comparison of maximum penetration depths measured on Ti-2 specimens with Fe content 0.078 wt% [15] and 0.107 wt%, respectively

## Conclusions

From the experimental results, the following conclusions can be drawn:

1. Crevice corrosion was mainly driven by internal proton reduction, i.e., more than 70%; external O<sub>2</sub> reduction on the counter electrode only contributed less than 30% of the corrosion processes.

2. Crevice corrosion was most likely to occur around the periphery of the crevice former and more likely to spread laterally across the metal surface than to penetrate deeper into the metal.
3. During crevice corrosion, absorbed hydrogen was accumulated throughout propagation, but the absorption efficiency did not change much, suggesting the hydrogen absorption process might be controlled by a diffusion step.
4. The iron content and distribution have a marked effect on the damage function (maximum penetration depth as a function of time). Iron present in intermetallics appears to suppress the propagation rate and limit the maximum depths of penetration.

### Reference

1. J.J. Noël, M.G. Bailey, J.P. Crosthwaite, B.M. Ikeda, S.R. Ryan, D.W. Shoesmith, "Hydrogen Absorption by Grade-2 Titanium", AECL-11608, COG-96-249
2. N.E. Paton, J.C. Williams, "Effect of Hydrogen on Titanium and Its Alloys", in *Hydrogen in Metals*, Bernstein, I.M. and Tompson, A.W. eds., American Society for Metals, p. 409-431
3. R.W. Schutz, *Corrosion* 59, 12 (2003): p. 1048-1050
4. R.S. Glass, *Electrochimica Acta*, 28, 11(1983): p.1507-1513
5. T. Watanabe, T. Shindo, H. Naito, "Effect of Iron Content in the Breakdown Potential for Pitting of Titanium in NaCl Solutions," Sixth World Conference on Titanium: Cannes, June 6-9, 1988. P. Lacombe, R. Tricot, G. Beranger, eds. IV, 1735-1740
6. B.M. Ikeda, R.C. Styles, M.G. Bailey, D.W. Shoesmith, "The Effect of Material Purity on Crevice Corrosion of Titanium in NaCl Solution," *Proceedings of the Symposium on Compatibility of Biomedical Implants*, (San Francisco, California, 1994), P. Kovacs, N.S. Istephanous, eds. Volume 94-15, 368-380
7. R.W. Schutz, J.S. Grauman, J.A. Hall, "Effect of Solid Solution Iron in the Corrosion Behaviour of Titanium," *Titanium, Science and Technology: Proceedings of the Fifth International Conference on Titanium*, Congress Center, Munich, FRG, September 10-14, 1984, G. Lutjering, U. Zwickler, W. Bunk, eds. 4, 2617-2624
8. R.W. Schutz, D.E. Thomas, "Corrosion of Titanium and Titanium Alloys," *Corrosion*, 13, ASM Handbook (1987): p. 669-706
9. I.I. Phillips, P. Poole and L.L. Shreir; *Corrosion Science*, vol.14 (1974) 553
10. T. Okada, *Electrochimica Acta*, 28, 8 (1983): p. 1113-1120
11. D.W. Shoesmith, F. Hua, K. Mon, G. De, P. Pasupathi, G. Gordon, "Hydrogen Induced Cracking of Titanium Alloys in Environments Anticipated in Yucca Mountain Nuclear Waste Repository", *CORROSION/2005*, paper no. 05582 (Houston, TX: NACE International, 2005)
12. Z. Qin and D.W. Shoesmith, "Lifetime Model for Ti-7 Drip Shields within the Yucca Mountain Repository", *Proc. of NACE Northern Area Eastern Conf.*, 2003.
13. J.J. Noël, *The Electrochemistry of Titanium Corrosion*, Ph. D. thesis, 1999
14. X. He, J.J. Noël, and D.W. Shoesmith; *Journal of the electrochemical society*; 149(9) (2002) p.440
15. X. He, *Effects of Temperature, Impurities, and Alloying Elements on the Crevice Corrosion of Alpha Titanium Alloys*, Ph. D. thesis, 2003